








# An Efficient Method for the Computation of Electromagnetic Fields Associated With Tortuous Lightning Channels

Massimo Brignone , Martino Nicora , *Student Member, IEEE*, Daniele Mestriner , *Member, IEEE*, Renato Procopio , *Senior Member, IEEE*, Carlo Petrarca , Alessandro Formisano , *Senior Member, IEEE*, Sami Barmada , *Senior Member, IEEE*, and Federico Delfino, *Member, IEEE*

**Abstract**—Lightning electromagnetic (EM) fields are typically computed by assuming the current propagation within a straight vertical channel of negligible cross section. However, it is well known that the lightning path is tortuous and this can significantly affect the radiated fields and the lightning-induced voltages on power lines. Lupò *et al.* (2000) proposed an analytical method evaluating the EM fields radiated by a tortuous channel assuming a step current source; to consider an arbitrary (realistic) current source, a slow-converging convolution integral was applied. The aim of this article is to reduce the computation time of such procedure by extending to the tortuous channel case the approach proposed by Brignone *et al.* (2021) for the evaluation of the lightning EM fields with arbitrary current source, originally developed for a straight vertical channel. The performances of the present method are evaluated by means of comparison with the solution proposed by Lupò *et al.* (2000), showing an excellent agreement with a significant reduction of the CPU effort. This in principle will allow the computation of lightning-induced overvoltages at both individual and statistical level without a prohibitive computational effort.

**Index Terms**—Computation time, lightning channel tortuosity, lightning electromagnetic fields.

## I. INTRODUCTION

**L**IGHTNING is one of the most dangerous natural phenomena, able to produce high impacts and damage even though its hazard perception is low. For this reason, both ground and air discharges have been intensively studied. In particular, cloud-to-ground discharges have received great interest in the

scientific literature, since they represent a significant risk for human beings, animals, civil structures, and power and communication infrastructures. On the other hand, intracloud and cloud-to-cloud events are important issues affecting aircraft safety; actually, lightning hazard is expected to increase with the development of aircraft technology, i.e., ever-more sophisticated on-board electronics and low-conducting carbon-fiber composite reinforcements reducing the shielding effect [1].

Lightning electromagnetic (EM) fields have been deeply investigated to perform the risk assessment of electric and electronic systems. The cloud-to-ground EM fields computation has usually been achieved by assuming the lightning current propagating within a straight vertical channel of negligible cross section above a perfectly conducting plane modeling the ground (e.g., [2]–[4]).

Although simple and widely adopted, such model lacks a realistic representation of some features of the lightning physics. Actually, it is known that lightning discharges are affected by tortuosity on a scale from less than 1 m to over 1 km with a mean absolute value of the channel direction azimuth of about  $16^\circ$  [5]. The radiated EM fields exhibit a fine structure with a jagged waveform and periodical phenomena at frequencies of engineering interest [6]. Moreover, intra-cloud and cloud-to-cloud discharges cannot be described by the vertical channel model since they are made of a number of channels with different slope and height above the ground [7].

The effects of the tortuous channel representation on the radiated EM fields have been investigated in some studies. In [8] the authors reported that, due to the presence of horizontal discharge components, the tortuous channel radiates at still higher frequencies with respect to the straight vertical channel that is characterized by a very large frequency (VLF) spectrum. The authors of [9], adopting a simple approach, found that in the frequency-domain the tortuous channel far-field waveform has larger amplitudes at frequencies above 100 kHz. Then, the authors of [10] modeled the lightning discharge as a fractal object and aimed to conclude that the radiated EM fields are fractals characterized by the same fractal dimension of the channel. Furthermore, it has been shown that tortuous channel, radiating as a fractal antenna, at high altitudes generates EM fields with spatially nonuniform intensity, contrarily to simple dipole antennas (e.g., [11]). In [12], by means of the Numerical

Manuscript received 28 October 2021; revised 29 April 2022; accepted 17 June 2022. (*Corresponding author: Martino Nicora.*)

Massimo Brignone, Martino Nicora, Daniele Mestriner, Renato Procopio, and Federico Delfino are with the ICT and Electrical Engineering Department, University of Genoa, I-16145 Genoa, Italy (e-mail: massimo.brignone@unige.it; martino.nicora@edu.unige.it; daniele.mestriner@edu.unige.it; renato.procopio@unige.it; federico.delfino@unige.it).

Carlo Petrarca is with the Department of Electrical Engineering, University of Naples Federico II, I-80125 Naples, Italy (e-mail: carlo.petrarca@unina.it).

Alessandro Formisano is with the Department of Engineering, Università della Campania Luigi Vanvitelli, I-81031 Aversa, Italy (e-mail: alessandro.formisano@unicampania.it).

Sami Barmada is with the School of Engineering, University of Pisa, I-56122 Pisa, Italy (e-mail: sami.barmada@unipi.it).

This article has supplementary material provided by the authors and color versions of one or more figures available at <https://doi.org/10.1109/TEMC.2022.3186726>.

Digital Object Identifier 10.1109/TEMC.2022.3186726

Electromagnetics Code NEC-4.1, it was found that also for very close distances and fast current rise times, the channel tortuosity can induce large EM fields variations.

All the above-mentioned studies adopt the far-field or a moment-based approximation. Lupò *et al.* [13], [14] were the first to introduce an analytical method with no mathematical approximation and able to evaluate the EM fields radiated by a tortuous channel by superimposing the contributes given by discharge currents traveling along a straight channel portion with arbitrary slope and height above the ground. They treated the problem with a unit step current pulse and suggested to compute the EM fields due to an arbitrary current source by superimposing the components due to current pulses of arbitrarily small width and performing a convolution integral. The adoption of an accurate current source is essential for the fields evaluation; therefore, for both measured and simulated lightning currents (see, e.g., the engineering return stroke models [15]) the approach proposed in [13] and [14] requires a remarkable computational effort, mainly due to the convolution integral.

The aim of this article is to provide a semianalytical method that allows us to evaluate the EM fields associated with a tortuous lightning channel, maintaining the same accuracy as [13] and [14], but significantly reducing the computational effort required when dealing with arbitrary channel-base current waveforms. For such purpose, the approach proposed by Brignone *et al.* [16] for the computation of lightning EM fields with arbitrary current source, originally developed for a vertical channel, is adopted and extended to the tortuous channel case.

Low computation time is mandatory when lightning-induced overvoltages on distribution and transmission lines have to be evaluated; this becomes even more crucial when one has to evaluate the Lightning Performance of a power system, as it requires a Monte Carlo procedure involving thousands of overvoltage computations (e.g., [17], [18]). Actually, it has been shown that a more realistic channel representation can significantly affect the lightning-induced overvoltage evaluation. The authors of [19] stated that the overall inclination of the bottom few hundred meters of the lightning channel is the predominant effect of variation for both fields and induced voltage, in accordance with [20] and [21], whereas the small-scale tortuosity is responsible for the fields and voltage waveform fine structure at some hundreds of meters and beyond. Moreover, tortuosity can be significant for the overvoltage assessment also at statistical level [22].

It is worth stressing that the proposed method assumes a perfectly conducting ground. Although such an assumption is generally valid for practical soil conductivity values, it is known that the finite ground conductivity can be significant, especially for the radial component of the E-field generated by a straight vertical channel. However, the evaluation of the EM fields generated by a tortuous channel above a lossy ground would imply the numerical solution of the slowly converging Sommerfeld's integrals [23] or the extension of approximated methods (e.g., the Cooray–Rubinstein empirical correction [24], [25]) originally developed for the straight vertical channel case. To the best of the authors' knowledge, this complex topic has not been studied yet, and it may be an object of future research.

The rest of this article is organized as follows. Section II describes the proposed semianalytical method calculating the lightning EM fields accounting for the channel tortuosity. The tortuous channel geometry numerical generation procedure is reported in Section III together with the model assumptions and parameters. Section IV shows the simulation results and comparisons with the solution provided by Lupò *et al.* [13], [14], with particular focus on the computational advantages. Finally, Section V concludes this article.

## II. METHOD

This section aims at describing the proposed method for calculating the EM fields associated with the tortuous lightning channel. The procedure steps are summarized as follows.

- 1) Generate the geometry of the channel dividing it into  $N$  straight line portions with arbitrary slope and height above the ground and generate the channel image geometry.
- 2) For each single line portion of the channel and of its image, define a local reference frame linked with the global one by means of a suitable linear mapping, such that the local reference  $z$ -axis is aligned with the channel portion.
- 3) Compute the EM fields radiated by the single channel portion in the local reference frame.
- 4) Compute the above fields in the global reference frame applying the inverse linear mapping.
- 5) Compute the total EM fields by applying the superposition principle.

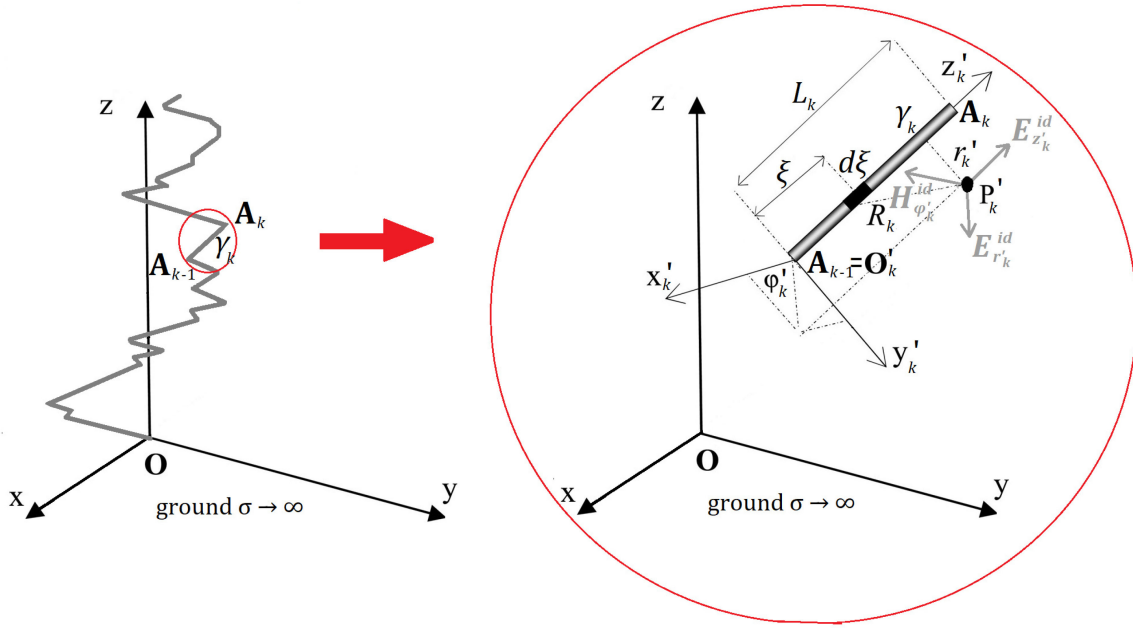
The main contribution of this article consists of adapting the procedure developed by Brignone *et al.* [16] to evaluate the EM fields of each channel portion, in order to improve the computational performances with respect to previously proposed studies [13], [14].

Such method allows us to consider a lightning return stroke characterized by an arbitrary channel-base current, in presence of either a perfectly conducting or a lossy ground, assuming the Transmission Line (TL) model [26] for the current propagation along the channel. The main idea consists of dividing the channel into intervals in which the distance between the field source point and the observation point can be approximated with a linear function of the time and of the spatial coordinates of both points.

In what follows, the definition of the local and global frames of the linear mapping between them and of the superposition principle application for the evaluation of the final EM fields appear in Section II-A. The analytical evaluation of the EM fields radiated by a single line portion of the tortuous lightning channel and of the image in the local reference frame, based on the approach proposed in [16], is the object of Section II-B.

### A. Merging Single Line Channel and Image Portion Contributions to the Total EM Fields

Let  $Oxyz$  be a spatial reference frame,  $\gamma \subset \mathbb{R}^3$  be the tortuous lightning channel,  $\mathbf{A}_0, \dots, \mathbf{A}_N \in \gamma$  be  $N + 1$  points such that  $\gamma = \bigcup_{k=1}^N \gamma_k$  with  $\gamma_h \cap \gamma_k = \emptyset$  for any  $h \neq k$ , and where  $\gamma_k : [0, L_k] \ni z' \mapsto \hat{\mathbf{v}}_k z' + \mathbf{A}_{k-1} \in \mathbb{R}^3$  is the segment with ends  $\mathbf{A}_{k-1}$  e  $\mathbf{A}_k$ . The segment length is defined as  $L_k = \|\mathbf{A}_k - \mathbf{A}_{k-1}\|_2$  (Euclidean distance), its directional unit vector


 Fig. 1. Tortuous discharge channel and detail of the straight channel portion  $\gamma_k$ .

as  $\hat{\mathbf{v}}_k = (\hat{v}_{k,x}, \hat{v}_{k,y}, \hat{v}_{k,z}) = \frac{\mathbf{A}_k - \mathbf{A}_{k-1}}{L_k}$  (Fig. 1). Defining

$$\hat{\mathbf{w}}_k = \begin{cases} \frac{(\hat{v}_{k,z}, 0, -\hat{v}_{k,x})}{\sqrt{\hat{v}_{k,x}^2 + \hat{v}_{k,z}^2}} & \text{if } \hat{v}_{k,x}^2 + \hat{v}_{k,z}^2 \neq 0 \\ (0, 0, -1) & \text{if } \hat{v}_{k,x} = \hat{v}_{k,z} = 0, \hat{v}_{k,y} > 0 \\ (0, 0, 1) & \text{if } \hat{v}_{k,x} = \hat{v}_{k,z} = 0, \hat{v}_{k,y} < 0 \end{cases} \quad (1)$$

$$\hat{\mathbf{q}}_k = \hat{\mathbf{v}}_k \times \hat{\mathbf{w}}_k \quad (2)$$

such that  $\{\hat{\mathbf{w}}_k, \hat{\mathbf{q}}_k, \hat{\mathbf{v}}_k\}$  is a right-hand orthonormal basis of  $\mathbb{R}^3$ , the linear transformation  $\Phi_k: \mathbb{R}^3 \rightarrow \mathbb{R}^3$  that maps each column vector  $\mathbf{v} \in \mathbb{R}^3$  to  $\Phi_k(\mathbf{v}) = \mathbf{M}_k \mathbf{v}$ , where

$$\mathbf{M}_k = \begin{pmatrix} \hat{w}_{k,x} & \hat{w}_{k,y} & \hat{w}_{k,z} \\ \hat{q}_{k,x} & \hat{q}_{k,y} & \hat{q}_{k,z} \\ \hat{v}_{k,x} & \hat{v}_{k,y} & \hat{v}_{k,z} \end{pmatrix} \quad (3)$$

is an isometry which satisfies  $\Phi_k(\hat{\mathbf{w}}_k) = \hat{\mathbf{e}}_{x'_k}$ ,  $\Phi_k(\hat{\mathbf{q}}_k) = \hat{\mathbf{e}}_{y'_k}$  e  $\Phi_k(\hat{\mathbf{v}}_k) = \hat{\mathbf{e}}_{z'_k}$ , with  $\hat{\mathbf{e}}_{\bullet}$  being the standard basis of  $\mathbb{R}^3$ . Therefore, it is possible to introduce the roto-translation

$$\Psi_k: \mathbb{R}^3 \ni \mathbf{v} \mapsto \mathbf{M}_k(\mathbf{v} - \mathbf{A}_{k-1}) \in \mathbb{R}^3 \quad (4)$$

such that in the new reference frame  $O'_k x'_k y'_k z'_k$ , defined as

$$(x'_k, y'_k, z'_k)^T = \Psi_k(x, y, z) \quad (5)$$

the origin  $O'_k$  coincides with the point  $\mathbf{A}_{k-1}$  and the unit vector  $\hat{\mathbf{v}}_k$  of the channel portion  $\gamma_k$  lays on the  $z'_k$ -axis. Introducing a cylindrical coordinates reference frame centered on  $O'_k$

$$x'_k = r'_k \cos \varphi'_k \quad y'_k = r'_k \sin \varphi'_k \quad z'_k = z'_k \quad (6)$$

and considering the relationship between cylindrical and Cartesian local coordinates

$$\begin{cases} \hat{\mathbf{e}}_{r'_k} = \cos \varphi'_k \hat{\mathbf{e}}_{x'_k} + \sin \varphi'_k \hat{\mathbf{e}}_{y'_k} \\ \hat{\mathbf{e}}_{\varphi'_k} = -\sin \varphi'_k \hat{\mathbf{e}}_{x'_k} + \cos \varphi'_k \hat{\mathbf{e}}_{y'_k} \\ \hat{\mathbf{e}}_{z'_k} = \hat{\mathbf{e}}_{r'_k} \times \hat{\mathbf{e}}_{\varphi'_k} \end{cases} \quad (7)$$

one can state that, in the local reference frame  $O'_k x'_k y'_k z'_k$ , the only nonzero component of the magnetic field radiated in vacuum by the channel portion  $\gamma_k$  is the azimuthal component  $H_{\varphi'_k}^{id} \hat{\mathbf{e}}_{\varphi'_k}$ . Assuming a perfectly conducting ground and adapting the well-known expression proposed in [27] for a vertical lightning channel, it results that

$$H_{\varphi'_k}^{id}(r'_k, z'_k, t) = \frac{1}{4\pi} \int_0^{L_k} \frac{r'}{R_k^3(\xi)} i_k \left( \xi, t - \frac{R_k(\xi)}{c_0} \right) + \frac{r'_k}{c_0 R_k^2(\xi)} \frac{\partial}{\partial t} i_k \left( \xi, t - \frac{R_k(\xi)}{c_0} \right) d\xi \quad (8)$$

where

$$R_k(\xi) := \sqrt{r'_k{}^2 + (z'_k - \xi)^2} \quad (9)$$

is the distance between the source and the observation point,  $c_0$  and  $v \leq c_0$  are the speed of light in vacuum and the return stroke speed, respectively, and  $i_k$  is the current propagating in the channel.  $\forall \xi \in [0, L_k]$ , the current is assumed to be

$$i_k(\xi, \tau) = i_0 \left( \tau - \frac{\sum_{j=0}^{k-1} L_j}{v} - \frac{\xi}{v} \right) \cdot \mathbb{1} \left( \tau - \frac{\sum_{j=0}^{k-1} L_j}{v} - \frac{\xi}{v} \right) \cdot \mathcal{P} \left( \sum_{j=0}^{k-1} L_j + \xi \right) \quad (10)$$

being  $\mathbb{1}$  the Heaviside function,  $L_0 = 0$ , and  $\mathcal{P}$  the attenuation function [28]. In the following, the TL engineering model [26] is assumed, i.e.,  $\mathcal{P}(\cdot) = 1$ . It should be noted that the proposed procedure could in principle be extended to other transmission line type engineering models for the propagation of the lightning current along the channel, e.g., the MTLE model [29]. However, this would considerably complicate the analytical computation of integrals. Furthermore, the engineering models have been validated through experimental campaigns, but they all assume a straight vertical channel; thus, a careful study regarding the extension of such models to the case of tortuous channels should first be conducted. Once this aspect has been verified, one could first of all try to approximate the attenuation function with a piece-wise constant function. Each channel segment would involve the current at the base of the channel multiplied by a different constant, so there would be no further complications in the evaluation of the integrals, with respect to what is shown in the following.

In the local reference frame, the electric field radiated in vacuum by the channel portion  $\gamma_k$  has only the radial component  $E_{r'_k}^{id} \hat{\mathbf{e}}_{\varphi'_k}$  and the vertical component  $E_{z'_k}^{id} \hat{\mathbf{e}}_{z'_k}$ . Switching from cylindrical to Cartesian coordinates, it results that

$$\mathbf{H}_k^{id}(P'_k, t) = H_{\varphi'_k}^{id}(r'_k, z'_k, t) \left( -\sin \varphi'_k \hat{\mathbf{e}}_{x'_k} + \cos \varphi'_k \hat{\mathbf{e}}_{y'_k} \right) \quad (11)$$

$$\begin{aligned} \mathbf{E}_k^{id}(P'_k, t) &= E_{\varphi'_k}^{id}(r'_k, z'_k, t) \left( \cos \varphi'_k \hat{\mathbf{e}}_{x'_k} + \sin \varphi'_k \hat{\mathbf{e}}_{y'_k} \right) \\ &+ E_{z'_k}^{id}(r'_k, z'_k, t) \hat{\mathbf{e}}_{z'_k} \end{aligned} \quad (12)$$

where the observation point in the local cylindrical reference frame coordinates is  $P'_k = (r'_k, \varphi'_k, z'_k)$ . Therefore, in the global reference frame  $Oxyz$ , the EM fields radiated in vacuum by the channel portion  $\gamma_k$  observed in  $P(x, y, z)$ , expressed in Cartesian global coordinates, are given by

$$\mathbf{H}_k^{id}(P, t) = \mathbf{M}_k^T \mathbf{H}_k^{id}(\Psi_k(P), t) \quad (13)$$

$$\mathbf{E}_k^{id}(P, t) = \mathbf{M}_k^T \mathbf{E}_k^{id}(\Psi_k(P), t). \quad (14)$$

The image  $\gamma_-$  of the channel  $\gamma$ , can be obtained by symmetry with respect to the ground, i.e., by introducing  $N$  segments  $\gamma_{-k} : [0, L_k] \in z' \mapsto \hat{\mathbf{v}}_{-k} z' + \tilde{\mathbf{A}}_{k-1} \in \mathbb{R}^3$  where  $\tilde{\mathbf{A}}_k = (A_{k,x}, A_{k,y}, -A_{k,z})$  and  $\hat{\mathbf{v}}_{-k} = \frac{\tilde{\mathbf{A}}_k - \tilde{\mathbf{A}}_{k-1}}{L_k} = (\hat{v}_{k,x}, \hat{v}_{k,y}, -\hat{v}_{k,z})$ . In the image channel, the current propagates in the opposite direction with respect to the source one. Thus, by applying the superposition principle, the total fields are given by

$$\mathbf{H}^{id}(P, t) = \sum_{k=1}^N (\mathbf{H}_k^{id}(P, t) - \mathbf{H}_{-k}^{id}(P, t)) \quad (15)$$

$$\mathbf{E}^{id}(P, t) = \sum_{k=1}^N (\mathbf{E}_k^{id}(P, t) - \mathbf{E}_{-k}^{id}(P, t)). \quad (16)$$

## B. Analytical Evaluation of the EM Fields Radiated by a Single Line Portion of the Tortuous Lightning Channel in the Local Reference Frame

The extension of the analytical method proposed in [16] from the vertical to the tortuous channel case has required some adjustments.

- 1) Contrary to the vertical case, by considering a single line portion of the tortuous channel, the propagating current always reaches its top.
- 2) For the vertical case, the observation point height  $z$  (typically,  $\sim 10$  m) is much lower than the channel height (typically,  $\sim 8$  km); considering a single line portion of the tortuous channel, its length may be lower than  $z$  in the local reference frame.
- 3) For the vertical case, the channel and its image can be treated jointly; for the tortuous channel, each single-line channel portion should be treated separately from its image since they are not aligned and consequently there is no local reference frame such that they both result vertical.

1) *Magnetic Field:* let  $L > 0$  be the length of the single line portion of the tortuous lightning channel in the local reference frame (i.e., a vertical radiator),  $i_0$  and  $i'_0$  be the current waveform at the base of the vertical radiator and its time derivative, respectively. In the following,  $i_0$  is assumed to have at least a continuous function and  $i_0(t) = 0$  for any  $t < 0$ .

Assuming a perfectly conducting ground and the TL engineering model [26] for the current, the azimuthal component of the magnetic field (ideal) in the vacuum, at distance  $r$ , height  $z$ , at time  $t$  satisfies

$$\begin{aligned} H_{\varphi}^{id}(r, z, t) &= \frac{r}{4\pi} \int_0^L \left[ \frac{1}{R^3(z')} i_0 \left( t - \frac{R(z')}{c_0} - \frac{z'}{v} \right) \right. \\ &\quad \left. + \frac{1}{c_0 R^2(z')} i'_0 \left( t - \frac{R(z')}{c_0} - \frac{z'}{v} \right) \right] dz' \end{aligned} \quad (17)$$

where

$$R(z') := \sqrt{r^2 + (z - z')^2}. \quad (18)$$

Integrating by parts and recalling the continuity of  $i_0$ , one has

$$\begin{aligned} &\int_0^L \frac{1}{R^3(z')} i_0 \left( t - \frac{R(z')}{c_0} - \frac{z'}{v} \right) dz' \\ &= \frac{L - z}{r^2 R(L)} i_0 \left( t - \frac{R(L)}{c_0} - \frac{L}{v} \right) + \frac{z}{r^2 R(0)} i_0 \left( t - \frac{R(0)}{c_0} \right) \\ &+ \int_0^L \frac{z' - z}{r^2 R(z')} i'_0 \left( t - \frac{R(z')}{c_0} - \frac{z'}{v} \right) \cdot \left( \frac{z' - z}{c_0 R(z')} + \frac{1}{v} \right) dz'. \end{aligned} \quad (19)$$

Therefore, (17) becomes

$$\begin{aligned} H_{\varphi}^{id}(r, z, t) &= \frac{r}{4\pi} \left( \frac{L - z}{r^2 R(L)} i_0 \left( t - \frac{R(L)}{c_0} - \frac{L}{v} \right) \right. \\ &\quad \left. + \frac{z}{r^2 R(0)} i_0 \left( t - \frac{R(0)}{c_0} \right) \right) \\ &+ \frac{1}{4\pi r} \int_0^L \left[ \frac{1}{c_0} + \frac{z' - z}{v R(z')} \right] i'_0 \left( t - \frac{R(z')}{c_0} - \frac{z'}{v} \right) dz'. \end{aligned} \quad (20)$$

Applying the fundamental theorem of integral calculus, one can manipulate the integral component of  $H_\varphi^{id}$  in (20) in order to get

$$\begin{aligned} H_\varphi^{id}(r, z, t) &= \frac{1}{4\pi r} \left( \left( \frac{L-z}{R(L)} - \frac{c_0}{v} \right) i_0 \left( t - \frac{R(L)}{c_0} - \frac{L}{v} \right) \right. \\ &+ \left. \left( \frac{z}{R(0)} + \frac{c_0}{v} \right) i_0 \left( t - \frac{R(0)}{c_0} \right) \right) \\ &+ \frac{c_0}{4\pi r} \left( \frac{1}{c_0^2} - \frac{1}{v^2} \right) I(r, z, t) \end{aligned} \quad (21)$$

in which

$$\begin{aligned} I(r, z, t) &= \int_0^L i_0' \left( t - \frac{R(z')}{c_0} - \frac{z'}{v} \right) dz \\ &= r \int_{-\frac{z}{r}}^{\frac{L-z}{r}} i_0' \left( t - \frac{r}{c_0} f(x) - \frac{z+rx}{v} \right) dx \end{aligned} \quad (22)$$

where the change of variable  $x = (z' - z)/r$  is used and  $f : \mathbb{R} \ni x \mapsto \sqrt{1+x^2} \in \mathbb{R}$ .

It is worth observing that, comparing (21) with (6) provided in [16] for the vertical channel, here the expression is more complex due to the considerations made at the beginning of this section.

Furthermore, while for the vertical case  $z$  is certainly much lower than the channel height, here it is mandatory to distinguish between  $L > z$  and  $L < z$  and to consider both cases, which determines some differences with respect to [16] in the evaluation of  $I$ .

To provide a semianalytical formula for  $I$ , it is useful to introduce a piecewise linear approximation of  $f$  such that

$$f(x) \simeq \tilde{f}(x) = \begin{cases} a_1|x| + b_1 & \alpha_0 \leq |x| \leq \alpha_1 \\ \vdots & \\ a_N|x| + b_N & \alpha_{N-1} \leq |x| \leq \alpha_N \end{cases} \quad (23)$$

where  $\alpha_0 = 0$ , while  $a_i$ ,  $b_i$  and  $\alpha_i$  ( $i = 1, \dots, N$ ) are chosen so as to ensure  $f(\alpha_i) = \tilde{f}(\alpha_i)$  for each  $i = 0, \dots, N$ . See [16] for details and for a physical interpretation of the whole method. This way, one has that

$$\begin{aligned} I(r, z, t) &\simeq \tilde{I}(r, z, t) \\ &:= r \int_{-\frac{z}{r}}^{\frac{L-z}{r}} i_0' \left( t - \frac{r}{c_0} \tilde{f}(x) - \frac{z+rx}{v} \right) dx. \end{aligned} \quad (24)$$

The advantage of using  $\tilde{I}$  instead of  $I$  is that in the approximate version the argument of  $i_0'$  is piecewise linear in the integration variable, making the integral analytically solvable. Due to the presence of the absolute value in  $\tilde{f}$ , to obtain an explicit formula for  $\tilde{I}$ , it is necessary to split  $\tilde{I}$  into the sum of two integrals (the first one, called  $\tilde{I}_1$ , on the negative part of the integration domain and the second, denoted by  $\tilde{I}_2$ , on the positive one), i.e.,

$$\begin{aligned} \tilde{I}(r, z, t) &= \tilde{I}_1(r, z, t) + \tilde{I}_2(r, z, t) \\ &= r \int_{x_{1,\min}}^{x_{1,\max}} i_0' (t - g(x)) dx \end{aligned}$$

$$+ r \int_{x_{2,\min}}^{x_{2,\max}} i_0' (t - g(x)) dx \quad (25)$$

where

$$g(x) = \frac{r}{c_0} \tilde{f}(x) + \frac{z+rx}{v} \quad (26)$$

and

$$x_{1,\min} = \min \left\{ 0, -\frac{z}{r} \right\} = \frac{z_{1,\min}}{r} \quad (27)$$

$$x_{1,\max} = \min \left\{ 0, \frac{L-z}{r} \right\} = \frac{z_{1,\max}}{r} \quad (28)$$

$$x_{2,\min} = \max \left\{ 0, -\frac{z}{r} \right\} = \frac{z_{2,\min}}{r} \quad (29)$$

$$x_{2,\max} = \max \left\{ 0, \frac{L-z}{r} \right\} = \frac{z_{2,\max}}{r} \quad (30)$$

where  $z_{1,\min} = \min\{0, -z\}$ ,  $z_{1,\max} = \min\{0, L-z\}$ ,  $z_{2,\min} = \max\{0, -z\}$  and  $z_{2,\max} = \max\{0, L-z\}$ .

It is worth noting that

- 1) if  $z \geq L \implies x_{2,\min} = x_{2,\max} = 0$
- 2) if  $z \leq 0 \implies x_{1,\min} = x_{1,\max} = 0$

Using simple algebraic computation and substitution integral rules, one gets  $\tilde{I}_1$  and  $\tilde{I}_2$  as follows (see [16] for details). As regards the expression of  $\tilde{I}_1$  one gets

$$\tilde{I}_1(r, z, t) = \begin{cases} -A_{1,h_1} i_0(t - t_{1,\min}) \\ \quad + \sum_{j=h_2}^{h_1-1} (A_{1,j+1} - A_{1,j}) i_0(t - t_j^{s,1}) \\ \quad + A_{1,h_2} i_0(t - t_{1,\max}) & z > 0 \\ 0 & z \leq 0. \end{cases} \quad (31)$$

Quantities appearing in (31) can be computed as follows: if  $z$  is positive, from (27) it results  $x_{1,\min} = -z/r$  and, from (23), there exist  $h_1, h_2 \in \{1, \dots, N\}$  such that

$$\begin{aligned} -\alpha_{h_1} &\leq x_{1,\min} < -\alpha_{h_1-1} \leq \dots \leq -\alpha_{h_2} \leq \\ &\leq x_{1,\max} \leq -\alpha_{h_2-1} \leq \dots \leq \alpha_0 = 0. \end{aligned} \quad (32)$$

Moreover, the time sequence  $t_{1,j}$  satisfies

$$\begin{aligned} t_{1,h_1} &\leq t_{1,\min} \leq t_{1,h_1-1} \leq \dots \leq t_{1,h_2} \leq \\ &\leq t_{1,\max} \leq t_{1,h_2-1} \leq \dots \leq t_{1,0} \end{aligned} \quad (33)$$

where  $\forall i = 1, \dots, N$ ,

$$t_{1,\min} = g(x_{1,\min}) = \frac{a_{h_1} z}{c_0} + \frac{b_{h_1} r}{c_0} \quad (34)$$

$$\begin{aligned} t_{1,\max} &= g(x_{1,\max}) = \\ &= \left( \frac{a_{h_2}}{c_0} - \frac{1}{v} \right) (-z_{1,\max}) + \frac{r b_{h_2}}{c_0} + \frac{z}{v} \end{aligned} \quad (35)$$

$$t_{1,i} = g(-\alpha_i) = r \left( \frac{a_i}{c_0} - \frac{1}{v} \right) \alpha_i + \frac{r b_i}{c_0} + \frac{z}{v} \quad (36)$$

$$t_{1,0} = g(0) = \frac{r}{c_0} + \frac{z}{v}. \quad (37)$$

Finally, quantities  $A_{1,j}$  are given by

$$A_{1,j} = \left( \frac{a_j}{c_0} - \frac{1}{v} \right)^{-1}. \quad (38)$$

Similarly, for the expression of  $\tilde{I}_2$  one gets

$$\tilde{I}_2(r, z, t) = \begin{cases} A_{2,h_3} i_0(t - t_{2,\min}) \\ \quad + \sum_{j=h_3}^{h_4-1} (A_{2,j+1} - A_{2,j}) i_0(t - t_{2,j}) + \\ \quad - A_{2,h_4} i_0(t - t_{2,\max}) & z < L \\ 0 & z \geq L. \end{cases} \quad (39)$$

Assuming  $z < L$ , from (30) it results  $x_{2,\max} = -\frac{L-z}{r}$  and, from (23), there are  $h_3, h_4 \in \{1, \dots, N\}$  such that

$$0 = \alpha_0 \leq \dots \leq \alpha_{h_3-1} \leq x_{2,\min} \leq \\ \leq \alpha_{h_3} \leq \dots \leq \alpha_{h_4-1} \leq x_{2,\max} \leq \alpha_{h_4} \leq \dots \leq \alpha_N. \quad (40)$$

The time sequence  $t_{2,j}$  satisfies

$$t_{2,0} \leq \dots \leq t_{2,h_3-1} \leq t_{2,\min} \leq t_{2,h_3} \leq \dots \leq t_{2,h_4-1} \leq \\ \leq t_{2,\max} \leq t_{2,h_4} \dots \leq t_{2,N} \quad (41)$$

where,  $\forall i = 1, \dots, N$ ,

$$t_{2,\min} = g(x_{2,\min}) = \left( \frac{a_{h_3}}{c_0} + \frac{1}{v} \right) z_{2,\min} + \frac{r b_{h_3}}{c_0} + \frac{z}{v} \quad (42)$$

$$t_{2,\max} = g(x_{2,\max}) = L \left( \frac{a_{h_4}}{c_0} + \frac{1}{v} \right) - \frac{a_{h_4} z}{c_0} + \frac{r b_{h_4}}{c_0} \quad (43)$$

$$t_{2,i} = g(\alpha_i) = r \left( \frac{a_i}{c_0} + \frac{1}{v} \right) \alpha_i + \frac{r b_i}{c_0} + \frac{z}{v} \quad (44)$$

$$t_{2,0} = g(\alpha_0) = \frac{r}{c_0} + \frac{z}{v} \quad (45)$$

and, finally, the quantities  $A_{2,j}$  are given by

$$A_{2,j} = \left( \frac{a_j}{c_0} + \frac{1}{v} \right)^{-1}. \quad (46)$$

Inserting (31) and (39) into (25) and then in (21) one obtains the final semianalytical formula for  $H_\varphi^{id}$  that reads

$$H_\varphi^{id}(r, z, t) \\ = \frac{1}{4\pi r} \left( \frac{L-z}{R(L)} - \frac{c_0}{v} \right) i_0 \left( t - \frac{R(L)}{c_0} - \frac{L}{v} \right) \\ + \frac{1}{4\pi r} \left( \frac{z}{R(0)} + \frac{c_0}{v} \right) i_0 \left( t - \frac{R(0)}{c_0} \right) \\ + \frac{c_0}{4\pi r} \left( \frac{1}{c_0^2} - \frac{1}{v^2} \right) \left( \tilde{I}_1(r, z, t) + \tilde{I}_2(r, z, t) \right). \quad (47)$$

2) *Electric Field*: Maxwell's equations applied to a single vertical line radiator allow us to state that the radial and vertical components of the ideal electric field can be calculated as [30]

$$E_r^{id}(t) = -\mu_0 c_0^2 \int_0^t \frac{\partial H_\varphi^{id}}{\partial z} d\tau \quad (48)$$

$$E_z^{id}(t) = \mu_0 c_0^2 \int_0^t \frac{1}{r} \frac{\partial(r H_\varphi^{id})}{\partial r} d\tau \quad (49)$$

$\mu_0$  being the vacuum magnetic permeability. Hence, it is sufficient to derive the magnetic field with respect to either  $r$  and  $z$  and to integrate in time.

a) *Radial component  $E_r^{id}$  evaluation*: To perform the partial derivative  $\partial_z H_\varphi^{id}$  the contributions given by the four terms in (25) are separated. The first two addends derivation can be achieved by means of simple algebraic manipulations. Thus, all calculus details are omitted for the sake of brevity. On the other hand, the third and fourth addends require more attention since it is necessary to calculate  $\partial_z \tilde{I}_1$  and  $\partial_z \tilde{I}_2$ .

Therefore, deriving (31) with respect to  $z$  it results

$$\frac{\partial \tilde{I}_1}{\partial z}(r, z, t) \\ = \begin{cases} A_{1,h_1} B_{1,\min} i_0'(t - t_{1,\min}) \\ \quad - \sum_{j=h_2}^{h_1-1} (A_{1,j+1} - A_{1,j}) B_{1,j} i_0'(t - t_{1,j}) \\ \quad - A_{1,h_2} B_{1,\max} i_0'(t - t_{1,\max}) & z > 0 \\ 0 & z \leq 0 \end{cases} \quad (50)$$

where

$$B_{1,\min} = \frac{\partial t_{1,\min}}{\partial z} = \frac{a_{h_1}}{c_0} \quad (51)$$

$$B_{1,\max} = \frac{\partial t_{1,\max}}{\partial z} = \begin{cases} \frac{1}{v} & z \leq L \\ \frac{a_{h_2}}{c_0} & z > L \end{cases} \quad (52)$$

$$B_{1,i} = \frac{\partial t_{1,i}}{\partial z} = \frac{1}{v} \quad \forall i = 1, \dots, N. \quad (53)$$

Similarly, deriving (39) with respect to  $z$  one gets

$$\frac{\partial \tilde{I}_2}{\partial z}(r, z, t) \\ = \begin{cases} -A_{2,h_3} B_{2,\min} i_0'(t - t_{2,\min}) \\ \quad - \sum_{j=h_3}^{h_4-1} (A_{2,j+1} - A_{2,j}) B_j^{s,2} i_0'(t - t_{2,j}) \\ \quad + A_{2,h_4} B_{2,\max} i_0'(t - t_{2,\max}) & z < L \\ 0 & z \geq L \end{cases} \quad (54)$$

where

$$B_{2,\min} = \frac{\partial t_{2,\min}}{\partial z} = \begin{cases} -\frac{a_{h_3}}{c_0} & z < 0 \\ \frac{1}{v} & z \geq 0 \end{cases} \quad (55)$$

$$B_{2,\max} = \frac{\partial t_{2,\max}}{\partial z} = -\frac{a_{h_4}}{c_0} \quad (56)$$

$$B_{2,i} = \frac{\partial t_{2,i}}{\partial z} = \frac{1}{v} \quad \forall i = 1, \dots, N. \quad (57)$$

Finally, by merging all the contributions, (48) becomes

$$E_r^{id}(t) = \frac{-\mu_0 c_0^2}{4\pi r} \left\{ \frac{r^2}{(R(0))^3} \int_0^t i_0 \left( \tau - \frac{R(0)}{c_0} \right) d\tau \right. \\ - \frac{r^2}{(R(L))^3} \int_0^t i_0 \left( \tau - \frac{R(L)}{c_0} - \frac{L}{v} \right) d\tau \\ + \frac{L-z}{c_0 R(L)} \left( \frac{L-z}{R(L)} - \frac{c_0}{v} \right) i_0 \left( t - \frac{R(L)}{c_0} - \frac{L}{v} \right) \\ \left. - \frac{z}{c_0 R(0)} \left( \frac{z}{R(0)} + \frac{c_0}{v} \right) i_0 \left( t - \frac{R(0)}{c_0} \right) \right\}$$

$$+ c_0 \left( \frac{1}{c_0^2} - \frac{1}{v^2} \right) \left[ \frac{\partial \tilde{I}_1}{\partial z}(r, z, t) + \frac{\partial \tilde{I}_2}{\partial z}(r, z, t) \right] \quad (58)$$

Caution should be paid to the current integral terms appearing in (58). If the current at the base of the vertical radiator  $i_0$  does not admit an analytical primitive (due to its characteristic behaviour of vanishing at infinity), one possibility is to apply a Prony expansion, as performed in [31] and summarized in Appendix.

*b) Vertical component  $E_z^{id}$  evaluation:* Also in this case, to perform the partial derivative  $\partial_r(rH_\varphi^{id})$  the contribution given by the four addends in (25) are separated and the first two addends' derivation is omitted for the sake of brevity. The third and fourth addends contain  $\partial_r \tilde{I}_1$  and  $\partial_r \tilde{I}_2$ , respectively. As in the previous paragraph, deriving (31) with respect to  $r$  it results

$$\frac{\partial \tilde{I}_1}{\partial r}(r, z, t) = \begin{cases} A_{1,h_1} C_{1,\min} i_0'(t - t_{1,\min}) \\ - \sum_{j=h_2}^{h_1-1} (A_{1,j+1} - A_{1,j}) C_{1,j} i_0'(t - t_j^{s,1}) \\ - A_{1,h_2} C_{1,\max} i_0'(t - t_{1,\max}) & z > 0 \\ 0 & z \leq 0 \end{cases} \quad (59)$$

where  $\forall i = 1, \dots, N$ ,

$$C_{1,\min} = \frac{\partial t_{1,\min}}{\partial r} = \frac{b_{h_1}}{c_0} \quad (60)$$

$$C_{1,\max} = \frac{\partial t_{1,\max}}{\partial r} = \frac{b_{h_2}}{c_0} \quad (61)$$

$$C_{1,i} = \frac{\partial t_{1,i}}{\partial r} = \left( \frac{a_i}{c_0} - \frac{1}{v} \right) \alpha_i + \frac{b_i}{c_0}. \quad (62)$$

Similarly, deriving (39) with respect to  $r$  one gets

$$\frac{\partial \tilde{I}_2}{\partial r}(r, z, t) = \begin{cases} -A_{2,h_3} C_{2,\min} i_0'(t - t_{2,\min}) \\ - \sum_{j=h_3}^{h_4-1} (A_{2,j+1} - A_{2,j}) C_{2,j} i_0'(t - t_{2,j}) \\ + A_{2,h_4} C_{2,\max} i_0'(t - t_{2,\max}) & z < L \\ 0 & z \geq L \end{cases} \quad (63)$$

where  $\forall i = 1, \dots, N$ ,

$$C_{2,\min} = \frac{\partial t_{2,\min}}{\partial r} = \frac{b_{h_3}}{c_0} \quad (64)$$

$$C_{2,\max} = \frac{\partial t_{2,\max}}{\partial r} = \frac{b_{h_4}}{c_0} \quad (65)$$

$$C_{2,1} = \frac{\partial t_{2,1}}{\partial r} = \left( \frac{a_i}{c_0} + \frac{1}{v} \right) \alpha_i + \frac{b_i}{c_0}. \quad (66)$$

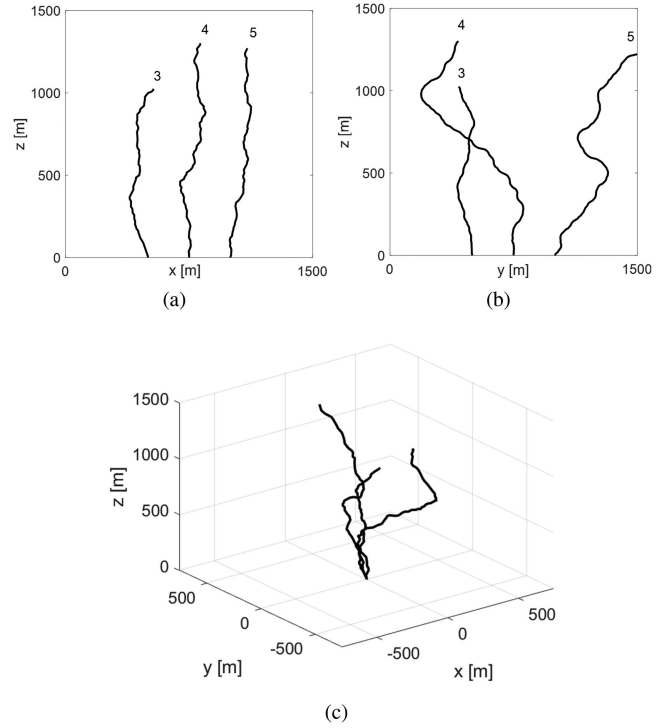


Fig. 2. Representation of the tortuous lightning channels used for the EM fields computations: (a)  $xz$ -view, (b)  $yz$ -view, and (c) 3D view.

Finally, by merging all the contributions, (49) becomes

$$E_z^{id}(t) = \frac{\mu_0 c_0^2}{4\pi r} \left\{ -\frac{r(L-z)}{(R(L))^3} \int_0^t i_0 \left( \tau - \frac{R(L)}{c_0} - \frac{L}{v} \right) d\tau \right. \\ - \frac{rz}{(R(0))^3} \int_0^t i_0 \left( \tau - \frac{R(0)}{c_0} \right) d\tau \\ - \frac{r}{c_0 R(L)} \left( \frac{L-z}{R(L)} - \frac{c_0}{v} \right) i_0 \left( t - \frac{R(L)}{c_0} - \frac{L}{v} \right) \\ - \frac{r}{c_0 R(0)} \left( \frac{z}{R(0)} + \frac{c_0}{v} \right) i_0 \left( t - \frac{R(0)}{c_0} \right) \\ \left. + c_0 \left( \frac{1}{c_0^2} - \frac{1}{v^2} \right) \left[ \frac{\partial \tilde{I}_1}{\partial r}(r, z, t) + \frac{\partial \tilde{I}_2}{\partial r}(r, z, t) \right] \right\}. \quad (67)$$

As in the previous paragraph, the current integral terms appearing in (67) can be treated according to the approach reported in the Appendix.

### III. TORTUOUS LIGHTNING CHANNELS GENERATION

An important and distinctive feature of lightning channels is their erratic nature, which is mainly determined by the leader process, which creates a conducting path between the cloud and ground and deposits charges along that path. The return stroke follows the leader formation, traverses the leader path, neutralizes the leader charge producing a peak current of some tens of kA, thus radiating EM energy in the surrounding space [32].

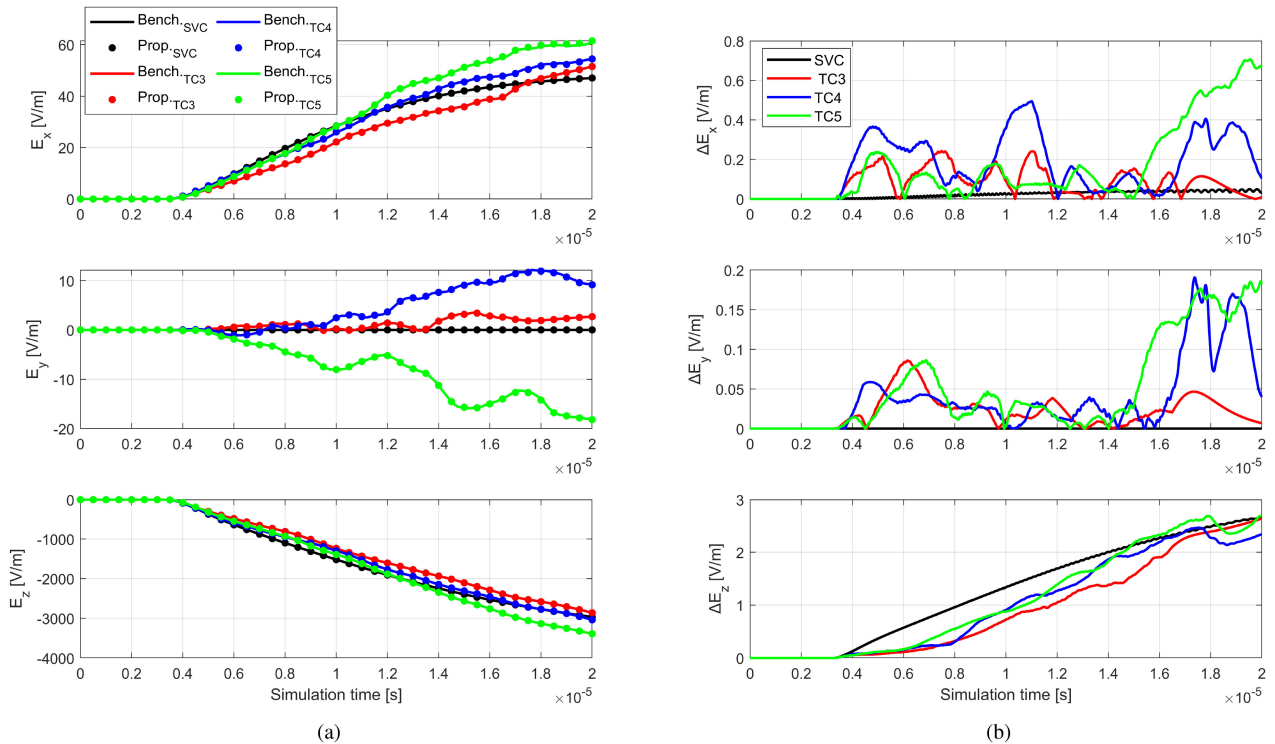


Fig. 3. (a) Time evolution of the  $E$ -field computed with the proposed method and that of [13] and [14], (b) and time evolution of the absolute difference  $\Delta E$  between the two approaches. A straight vertical channel (SVC) and three different tortuous ones (TC3, TC4, and TC5) are considered. Observation point (1000, 0, 10) m.

Lightning channels are therefore tortuous in nature and, from an engineering point of view, can be seen as composed of several segments, each with different slope and location above the ground, forming a piecewise linear chain.

Only a few pioneering papers tried to statistically characterize the irregular paths of lightning channels [8], [33]. In particular, Hill [8] described the technique adopted to measure the tortuosity of several natural lightning channels, while Idone and Orville [33] compared the geometrical characteristics of both triggered and natural flashes. The results obtained for the natural channels are in excellent agreement; in fact, the calculated mean absolute value of the deviation angle  $\Delta\Omega_m$  in moving from one segment of the path to the next is  $17.3^\circ$  for [8] and  $17.0^\circ$  for [33].

In this article, the data shown by Hill [8] and Idone and Orville [33] have been used in order to “artificially” create the 3-D lightning channels adopted for the numerical simulations. In particular, the procedure described in the following has been adopted: 1) the representation in  $xz$ -plane has been obtained by digitization of three photographed natural channels among those displayed in Fig. 2 of the paper by Idone and Orville [33], i.e., tortuous channels no. 3–5; 2) conversely, the representation in the  $yz$ -plane has been generated by randomly choosing the slope of the channel segments from a Gaussian distribution with mean value  $|\Delta\Omega_m| = 17.0^\circ$  and standard deviation  $\sigma_\Omega = 11.0^\circ$ . The average length  $L_m$  and the standard deviation  $\sigma_L$  of the resulting segments is different for each channel and equal to ( $L_m^3 = 5.6$  m,  $\sigma_L^3 = 3.3$  m), ( $L_m^4 = 10.3$  m,  $\sigma_L^4 = 1.9$  m), ( $L_m^5 = 23.7$  m,  $\sigma_L^5 = 11.6$  m), respectively.

The generated channels are shown in Fig. 2(a) ( $xz$ -view), (b) ( $yz$ -view), and (c) (3-D view). It is worth noting that the base of all channels adopted for the simulations is coincident with the origin of the  $Oxyz$ -reference frame, as shown in Fig. 2(c). The representation in Fig. 2(a) and (b) is only used for a better visualization of the channels and reproduces the way of representing channels adopted by Idone and Orville [33].

#### IV. RESULTS AND DISCUSSION

This section aims at presenting the results obtained with the proposed method for the lightning electromagnetic field computation associated with a tortuous channel. Such a method is implemented by assuming a perfectly conducting ground and the TL engineering model [26] for the current propagation. The channel-base current is assumed to be represented by a classical Heidler’s function [34] whose parameters are selected to reproduce the waveform of a typical first return stroke with a 30 kA current peak.

Lightning EM fields are calculated with both the proposed method and that of [13] and [14] at four different observation points  $P = (x, y, z)$ , i.e., (50, 0, 10) m, (50, 0, 100) m, (1000, 0, 10) m, (1000, 0, 100) m. Moreover, EM fields are calculated considering three different lightning channels shown in Fig. 2 and an 8 km straight vertical channel.

Fig. 3(a) depicts the time behavior of the three components of the electric field at (1000, 0, 10) m for the four different channels, i.e., the straight vertical channel (SVC), Tortuous Channel no. 3 (TC3), Tortuous Channel no. 4 (TC4), and Tortuous Channel



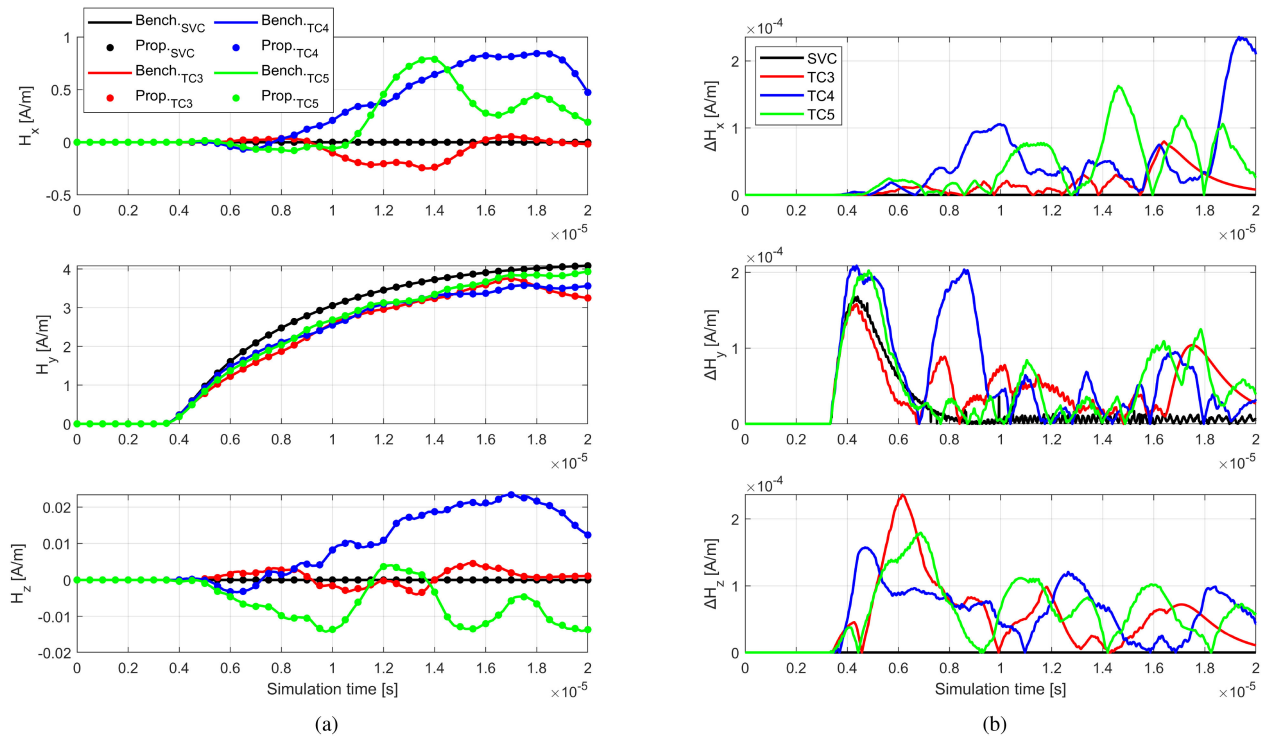


Fig. 4. (c) Time evolution of the  $H$ -field computed with the proposed method and that of [13] and [14], (b) and time evolution of the absolute difference  $\Delta H$  between the two approaches. A straight vertical channel (SVC) and three different tortuous ones (TC3, TC4, and TC5) are considered. Observation point  $(1000, 0, 10)$  m.

TABLE I  
CODES COMPARISON: MAXIMUM ABSOLUTE DIFFERENCE  $\Delta E_{max}$  ( $\Delta H_{max}$ ) BETWEEN ELECTRIC (MAGNETIC) FIELDS CALCULATED WITH THE PROPOSED METHOD AND WITH THAT OF [13] AND [14]

Observation point $P = (x, y, z)$	Straight vertical channel		Tortuous channel 3		Tortuous channel 4		Tortuous channel 5	
	$\Delta E_{max}$ [V/m]	$\Delta H_{max}$ [mA/m]	$\Delta E_{max}$ [V/m]	$\Delta H_{max}$ [mA/m]	$\Delta E_{max}$ [V/m]	$\Delta H_{max}$ [mA/m]	$\Delta E_{max}$ [V/m]	$\Delta H_{max}$ [mA/m]
(50, 0, 10) m	91.16	0.14	68.98	5.51	102.68	5.43	92.70	5.47
(50, 0, 100) m	87.88	0.16	48.22	1.24	109.39	1.24	55.70	1.57
(1000, 0, 10) m	2.66	0.17	2.64	0.24	2.47	0.24	2.69	0.20
(1000, 0, 100) m	2.64	0.17	2.62	0.16	2.59	0.17	3.14	0.22

no. 5 (TC5). The effects of channel tortuosity can be observed: the  $y$  component is nonzero and a jagged shape is exhibited, leading to an increase of the E-field derivative. Solid lines are obtained with the method of [13] and [14], while dots are obtained with the proposed method. Fig. 3(b) shows the time behavior of the three components of the absolute difference  $\Delta E$  between the  $E$ -field values computed with the two approaches. It can be observed that for all four channels  $\Delta E$  is two ( $x$  and  $y$  components) or three ( $z$  component) orders of magnitude smaller than the E-field.

Fig. 4 is the analogous of Fig. 3 for the  $H$ -field and the absolute difference  $\Delta H$ . In this case, for the tortuous channels the  $x$  and the  $z$  components of the H-field are nonzero and characterized by a jagged shape.  $\Delta H$  is two ( $z$  component) or four ( $x$  and  $y$  components) orders of magnitude smaller than the H-field.

EM fields waveshapes at the other considered observation points are not reported for the sake of brevity. However, an excellent agreement between the two methods is obtained at all observation points, as shown in Table I, which reports the

maximum absolute difference for both the electric field ( $\Delta E_{max}$ ) and the magnetic field ( $\Delta H_{max}$ ). Such quantities are defined as

$$\Delta E_{max} := \max \{ \max \{ \Delta E_x \}, \max \{ \Delta E_y \}, \max \{ \Delta E_z \} \} \quad (68)$$

$$\Delta H_{max} := \max \{ \max \{ \Delta H_x \}, \max \{ \Delta H_y \}, \max \{ \Delta H_z \} \} . \quad (69)$$

At  $(1000, 0, 100)$  m,  $E_z$  and all components of  $\Delta E$  are similar to those shown in Fig. 3 for the observation point  $(1000, 0, 10)$  m. On the other hand,  $E_x$  and  $E_y$  are of one order of magnitude higher. Regarding the magnetic field at  $(1000, 0, 100)$  m,  $H_x$ ,  $H_y$ , and all components of  $\Delta H$  are similar to those shown in Fig. 4 for the observation point  $(1000, 0, 10)$  m, while  $H_z$  is one order of magnitude higher.

At a closer distance from the channel, i.e., at  $(50, 0, 10)$  m and  $(50, 0, 100)$  m, the E-field magnitude is on the order of tens of

TABLE II  
CODES COMPARISON: COMPUTATION TIME [S]

Observation point $P = (x, y, z)$	Straight vertical channel		Tortuous channel 3		Tortuous channel 4		Tortuous channel 5	
	Bench. [13], [14]	Prop.	Bench. [13], [14]	Prop.	Bench. [13], [14]	Prop.	Bench. [13], [14]	Prop.
(50, 0, 10) m	3.86	0.08	4.60	1.48	3.69	1.06	2.36	0.51
(50, 0, 100) m	3.95	0.07	4.75	1.29	3.60	0.91	2.38	0.48
(1000, 0, 10) m	3.55	0.06	4.05	1.13	3.11	0.80	2.12	0.38
(1000, 0, 100) m	3.10	0.03	4.09	1.07	3.16	0.83	2.16	0.38

kV/m, while that of  $\Delta E$  is some tens of V/m. The H-field magnitude is on the order of units or tens of A/m, while  $\Delta H$  is always four orders of magnitude smaller than the corresponding H-field.

Table II reports the performance comparison between the proposed method and that of [13], [14]. One can observe that a 68%–82% decrease in CPU time can be achieved with the proposed approach for the calculation of the EM fields generated by tortuous channels. This significant code speed-up could be exploited to consider channel tortuosity in the assessment of lightning induced overvoltages without a prohibitive computational effort. Results have been obtained with a Microsoft Windows 10 PC equipped with 32 GB of RAM and an Intel Core i9-10885H CPU at 2.4 GHz.

## V. CONCLUSION

This contribution shows a semianalytical method for the computation of lightning electromagnetic fields associated with a tortuous channel, assuming a perfectly conducting ground and the Transmission Line model for the current propagation, but without any constraint on the waveform of the channel-base current. The proposed approach does not require the solution of any convolution integral. The method has been validated against a numerical one considering different channel geometries and different observation points. Comparison has shown an excellent agreement: considering a first return stroke with a 30-kA channel-base peak current, the E-field (H-field) absolute difference between the proposed method, and the benchmark method at a distance of 50 m from the channel is on the order of tens of V/m (units of mA/m), while it is on the order of units of V/m (tenths of mA/m) at a distance of 1000 m. The main advantages of the proposed approach consist in a significant reduction of the required CPU time: a 68–82% decrease has been obtained. This in principle will allow us to include channel tortuosity in procedures for the evaluation of lightning induced overvoltages at both individual and statistical level without a prohibitive computational effort.

## APPENDIX

In both electric field expressions reported in (58) and (67) for the radial and the vertical component, respectively, the following integral term appears:

$$\int_0^t i_0(\tau - \alpha) d\tau \quad (70)$$

with  $\alpha > 0$ . If the current  $i_0$  does not admit an analytical primitive, (70) cannot be solved analytically. However, following the approach proposed in [31], one possibility is to apply the Prony's expansion, i.e., to approximate  $i_0$  by means of a linear

combination of exponential functions. Thus, one assumes that there are  $N_G$  coefficients  $q_h, s_h \in \mathbb{C}$  such that

$$i_0(t) = \sum_{h=1}^{N_G} q_h \exp(s_h t) \mathbb{1}(t). \quad (71)$$

Observing that

$$\begin{aligned} \exp_0(t, s) &:= \int_0^t \exp(s(\tau - \alpha)) \mathbb{1}(\tau - \alpha) d\tau = \\ &= \begin{cases} \frac{1}{s} (\exp(s(t - \alpha)) - 1) \mathbb{1}(t - \alpha) & s \neq 0 \\ (t - \alpha) \mathbb{1}(\tau - \alpha) & s = 0 \end{cases} \end{aligned} \quad (72)$$

it is possible to write

$$\int_0^t i_0(\tau - \alpha) d\tau = \sum_{h=1}^{N_G} q_h \exp_0((t - \alpha), s_h). \quad (73)$$

## REFERENCES

- [1] J. Fisher, P. Hoole, K. Pirapaharan, S. Thirukumaran, and S. Hoole, "Three dimensional electric dipole model for lightning-aircraft electro-dynamics and its application to low flying aircraft," in *Proc. Int. Conf. Lightning Protection*, 2014, pp. 435–439.
- [2] M. A. Uman, "Lightning return stroke electric and magnetic fields," *J. Geophysical Res., Atmospheres*, vol. 90, no. D4, pp. 6121–6130, 1985.
- [3] M. Rubinstein and M. Uman, "Methods for calculating the electromagnetic fields from a known source distribution: Application to lightning," *IEEE Trans. Electromagn. Compat.*, vol. 31, no. 2, pp. 183–189, May 1989.
- [4] E. P. Krider, "On the electromagnetic fields, poyniting vector, and peak power radiated by lightning return strokes," *J. Geophysical Res., Atmospheres*, vol. 97, no. D14, pp. 15 913–15 917, 1992.
- [5] R. D. Hill, "Electromagnetic radiation from erratic paths of lightning strokes," *J. Geophysical Res. (1896–1977)*, vol. 74, no. 8, pp. 1922–1929, 1969.
- [6] C. D. Weidman and E. P. Krider, "The fine structure of lightning return stroke wave forms," *J. Geophysical Res., Oceans*, vol. 83, no. C12, pp. 6239–6247, 1978.
- [7] V. A. Rakov and M. A. Uman, *Lightning: Physics and Effects*. Cambridge, U.K.: Cambridge Univ. Press, 2003.
- [8] R. D. Hill, "Analysis of irregular paths of lightning channels," *J. Geophysical Res. (1896–1977)*, vol. 73, no. 6, pp. 1897–1906, 1968.
- [9] D. M. LeVine and R. Meneghini, "Simulation of radiation from lightning return strokes: The effects of tortuosity," *Radio Sci.*, vol. 13, no. 5, pp. 801–809, 1978.
- [10] G. Vecchi, D. Labate, and F. Canavero, "Fractal approach to lightning radiation on a tortuous channel," *Radio Sci.*, vol. 29, no. 4, pp. 691–704, 1994.
- [11] G. Milikh and J. A. Valdivia, "Model of gamma ray flashes due to fractal lightning," *Geophysical Res. Lett.*, vol. 26, no. 4, pp. 525–528, 1999.
- [12] J. G. Herrera and H. Torres, "Lightning electromagnetic fields associated to tortuous channels over a finitely conductive ground," in *Proc. 9th Int. Symp. Lightning Protection*, 2007.
- [13] G. Lupò, C. Petrarca, V. Tucci, and M. Vitelli, "EM fields associated with lightning channels: On the effect of tortuosity and branching," *IEEE Trans. Electromagn. Compat.*, vol. 42, no. 4, pp. 394–404, Nov. 2000.

- [14] G. Lupò, C. Petrarca, V. Tucci, and M. Vitelli, "EM fields generated by lightning channels with arbitrary location and slope," *IEEE Trans. Electromagn. Compat.*, vol. 42, no. 1, pp. 39–53, Feb. 2000.
- [15] C. A. Nucci, G. Diendorfer, M. A. Uman, F. Rachidi, M. Ianoz, and C. Mazzetti, "Lightning return stroke current models with specified channel-base current: A review and comparison," *J. Geophysical Res., Atmospheres*, vol. 95, no. D12, pp. 20 395–20 408, 1990.
- [16] M. Brignone *et al.*, "Analytical expressions for lightning electromagnetic fields with arbitrary channel-base current-Part I: Theory," *IEEE Trans. Electromagn. Compat.*, vol. 63, no. 2, pp. 525–533, Apr. 2021.
- [17] M. Brignone, F. Delfino, R. Procopio, M. Rossi, and F. Rachidi, "Evaluation of power system lightning performance-Part II: Application to an overhead distribution network," *IEEE Trans. Electromagn. Compat.*, vol. 59, no. 1, pp. 146–153, Feb. 2017.
- [18] M. Nicora *et al.*, "Estimation of the lightning performance of overhead lines accounting for different types of strokes and multiple strike points," *IEEE Trans. Electromagn. Compat.*, vol. 63, no. 6, pp. 2015–2023, Dec. 2021.
- [19] A. Andreotti, C. Petrarca, V. A. Rakov, and L. Verolino, "Calculation of voltages induced on overhead conductors by nonvertical lightning channels," *IEEE Trans. Electromagn. Compat.*, vol. 54, no. 4, pp. 860–870, Aug. 2012.
- [20] A. Sakakibara, "Calculation of induced voltages on overhead lines caused by inclined lightning studies," *IEEE Trans. Power Del.*, vol. 4, no. 1, pp. 683–693, Jan. 1989.
- [21] R. Moini, S. Sadeghi, B. Kordi, and F. Rachidi, "An antenna-theory approach for modeling inclined lightning return stroke channels," *Elect. Power Syst. Res.*, vol. 76, no. 11, pp. 945–952, 2006.
- [22] A. Andreotti, C. Petrarca, and A. Pierno, "On the effects of channel tortuosity in lightning-induced voltages assessment," *IEEE Trans. Electromagn. Compat.*, vol. 57, no. 5, pp. 1096–1102, Oct. 2015.
- [23] A. Sommerfeld, *Partial Differential Equations in Physics*. New York, NY, USA: Academic Press, 1949.
- [24] V. Cooray and V. Scuka, "Lightning-induced overvoltages in power lines: Validity of various approximations made in overvoltage calculations," *IEEE Trans. Electromagn. Compat.*, vol. 40, no. 4, pp. 355–363, Nov. 1998.
- [25] M. Rubinstein, "An approximate formula for the calculation of the horizontal electric field from lightning at close, intermediate, and long range," *IEEE Trans. Electromagn. Compat.*, vol. 38, no. 3, pp. 531–535, Aug. 1996.
- [26] M. A. Uman and D. K. McLain, "Magnetic field of lightning return stroke," *J. Geophysical Res. (1896–1977)*, vol. 74, no. 28, pp. 6899–6910, 1969.
- [27] F. Rachidi, C. Nucci, M. Ianoz, and C. Mazzetti, "Influence of a lossy ground on lightning-induced voltages on overhead lines," *IEEE Trans. Electromagn. Compat.*, vol. 38, no. 3, pp. 250–264, Aug. 1996.
- [28] V. Rakov and M. Uman, "Review and evaluation of lightning return stroke models including some aspects of their application," *IEEE Trans. Electromagn. Compat.*, vol. 40, no. 4, pp. 403–426, Nov. 1998.
- [29] C. Nucci, C. Mazzetti, F. Rachidi, and M. Ianoz, "On lightning return stroke models for LEMP calculations," in *Proc. 19th Int. Conf. Lightning Protection*, Graz, Austria, 1988.
- [30] C. Paul, *Analysis of Multiconductor Transmission Lines*. Hoboken, NJ, USA: Wiley, 2008.
- [31] F. Delfino, R. Procopio, M. Rossi, and F. Rachidi, "Prony series representation for the lightning channel base current," *IEEE Trans. Electromagn. Compat.*, vol. 54, no. 2, pp. 308–315, Apr. 2012.
- [32] H. Betz, U. Schumann, and P. Laroche, Eds., *Lightning: Principles, Instruments and Applications-Review of Modern Lightning Research*. Berlin, Germany: Springer, 2009.
- [33] V. P. Idone and R. E. Orville, "Channel tortuosity variation in florida triggered lightning," *Geophysical Res. Lett.*, vol. 15, no. 7, pp. 645–648, 1988.
- [34] H. Heidler, "Analytische blitzstromfunktion zur LEMP-berechnung," *Proc. 18th Int. Conf. Lightning Protection*, Munich, Germany, 1985, pp. 63–66.